Chitosan/hollow silica sphere nanocomposites for wound healing application

Ayşe Aslan
Department of Bioengineering, Gebze Technical University, Gebze, Kocaeli 41400, Turkey

Silviya Elanthikkal
Deanship of Scientific Research, Department of Nanomedicine, Institute for Research & Medical Consultations, Imam Abdulrahman Bin Faisal University, Dammam 31441, Saudi Arabia

Ayhan Bozkurt[a)]
Department of Biophysics, Institute for Research & Medical Consultations, Imam Abdulrahman Bin Faisal University, Dammam 31441, Saudi Arabia

(Received 15 July 2018; accepted 19 October 2018)

Chitosan is an important cationic biopolymer widely used in various biomedical applications such as wound care, drug delivery, biomaterial scaffolds, and tissue engineering. In this work, hollow silica sphere (HSS) nanoparticles with an average size of 400–450 nm (via TEM) were synthesized by sol–gel process and were epoxidized using epichlorohydrin. Then, chitosan was chemically bound to the epoxidized HSS to form a bionanocomposite, HSS-epoxy-CHI-X where X represents the percentage of chitosan in the sample. BET analysis showed that pure HSS has a specific surface area (A_{ss}) of around 4.8 m^2/g and adsorption average pore diameter of 10.18 nm. Bionanocomposites were characterized by FT-IR spectroscopy to confirm the bonding of chitosan on HSS nanoparticles. X-ray diffraction studies demonstrated that the amorphous character of the materials improved with the HSS content. Thermogravimetric analysis illustrated that at low temperatures, the thermal stability of bionanocomposites was higher than that of the sample with no chitosan in it. Scanning electron microscopic analysis results confirmed the homogenous distribution of HSS in the bionanocomposites. Considering the biological activity of chitosan and absorption characteristics of HSS, newly developed HSS-epoxy-CHI-X bionanocomposites were tested for wound healing by in vitro scratch assay using NIH 3T3 fibroblast cells. Among the bionanocomposites analyzed, HSS-epoxy-CHI-60 exhibited better performance where about 90% wound closure was observed for this sample after 21 h of exposure.

I. INTRODUCTION

Extensive studies are being conducted on the development of chitosan-based biomaterials for various biomedical applications such as wound healing, wound dressing, tissue engineering, and drug delivery. Chitosan-based materials can be easily processed in the form of gels, membranes, sponges, fibrils, beads, scaffolds, or nanoparticles.[1–3] Zhou et al.[4] prepared a composite nanofibrous mat from polyvinyl alcohol and carboxyethyl chitosan nanofibers via electro-spinning and studied the L 929 cell attachment and proliferation. The authors reported that this fibrous mat has the potential to be used as a wound dressing material for skin regeneration. In their later study, silk fibroin nanoparticles were also added and a composite fibrous mat having good biocompatibility and skin regeneration capacity was developed.[5] Nguyen et al.[6] developed a curcumin/chitosan/gelatin composite sponge having improved water uptake ability, wound closure, and antibacterial activity. In another study, chitosan hydrogel was prepared for wound dressing and cell viability tests were conducted using fibroblast cells isolated from rat skin.[7] The authors reported that chitosan hydrogel promoted cell adhesion and proliferation, and chitosan and its degradation by-products were found non-cytotoxic. Another group developed chitosan/polyethylene glycol diacrylate blend films for wound dressing application and evaluated the in vitro cytotoxicity of the films using L929 mouse fibroblasts. The material showed good biocompatibility and non-cytotoxicity.[8]

For decades, organic and/or inorganic nanomaterials such as polymers, dendrimers, liposomes, micelles, and materials based on carbon, iron oxide, silicon, silver, or gold with different morphologies such as nanotubes, nanowires, nanocapsules, nanofilms, and nanogels have been fabricated and explored as new platforms for diagnostic and therapeutic purposes.[9] Among the various inorganic nanoparticles, silica particles have attracted much interest because of their excellent chemical

[a)]Address all correspondence to this author.
e-mail: abozkurt@iau.edu.sa
DOI: 10.1557/jmr.2018.430

 © Materials Research Society 2018

https://doi.org/10.1557/jmr.2018.430 Published online by Cambridge University Press

stability, inert nature, thermal stability, low density, low toxicity, and biocompatibility. Silica nanoparticles show good compatibilities with other materials and can also be functionalized easily for chemically binding other active materials.

Over the past decades, a huge volume of research has been conducted on mesoporous silica nanoparticles (MSNs) and hollow silica sphere (HSS) nanoparticles. Because of their large surface area, stability, and biocompatibility, these silica nanoparticles found application in biomedical field, pharmaceutics, and biochemistry.[10,11] These particles are used as shield for enzymes or proteins, and as delivery vehicles for drugs because of their porous nature and greater loading efficiency.[12,13] A number of synthetic techniques exist in the literature for the production of silica nanoparticles.[14] Silica nanoparticles having the desired particle size, shape, porosity, and crystallinity can be generated by properly designing the appropriate synthetic route.[15,16]

Sol–gel process and template-assisted synthesis are the generally adopted methods for the production of HSSs. The form of nanoparticles can be changed using a shaped template or by adding various dopants as precursors, varying pH, or varying temperature during production. These hollow particles which can carry very bulky payloads or comprise cores may include desirable materials such as metals or various polymers.[10] Monodispersed phenyl groups-containing HSSs were generated by Hah et al.,[17] Wang et al.,[18] and Aslan et al.[19] without using any templates. These HSS nanospheres were soluble in organic solvents.

Combining HSS with smart biopolymers is an interesting approach which may be used in biomedical applications such as drug delivery and wound dressing. Fang et al. developed a pH-responsive drug carrier using chitosan-coated MSNs.[20] Drug-loaded MSN particles were added to the chitosan solution at pH 6 and stirred for 36 h, then centrifuged, washed, and dried. In another set, instead of MSN, methacryloxy propyl trimethoxysilane-coupled MSN was used and drug release was studied from both systems in a narrow pH range. The authors reported that chitosan-wrapped MSNs exhibited targeted drug release. A greater release of drug was observed at pH 6.8, the pH of inflammatory tissues and tumor cells, compared to pH 7.4, the pH of normal cells. It was noted that the material in which chitosan wrapped directly on to MSN showed better pH sensitivity than the material that contained a coupling agent.

For a material to be used in wound healing applications, it should be biocompatible, non-cytotoxic, and non-allergenic and should inhibit growth of microbial organisms. Chitosan possess all the above-mentioned characteristics. Silica materials have the capability to absorb wound exudates. Some researchers have investigated silica–chitosan combinations for hemostatic applications. Sun et al. fabricated a porous chitosan/kaolin composite microsphere through an inverse microemulsion process combined with thermally induced phase separation at −196 °C and found that these porous microspheres are a promising quick hemostat.[21]

In a recent work, a three-component system composed of chitosan, dopamine, and biosilica has been prepared to be used for rapid blood coagulation in hemostatic applications.[22] Although some naturally available silica has been investigated for hemostatic applications in combination with chitosan, the wound healing potential of synthetic HSS—chitosan bionanocomposites has not been studied.

In this work, we report the preparation and characterization of chitosan-functionalized HSSs by epoxidizing HSS and chemically binding chitosan onto the HSS to form HSS-epoxy-CHI-X where X represents the percentage (w/w) of chitosan in the bionanocomposite. The epoxidation of HSS via polymerization of glycidyl methacrylate (GMA) monomer has been reported in our previous article, where GMA monomer that contained an epoxy unit was polymerized on the surface of HSS.[19] However, in this study, epichlorohydrin was used to carry out direct epoxidation on the surface of HSS. In the second step, chitosan binding was achieved through a ring-opening reaction between the epoxy-functionalized HSS and chitosan. The developed materials were characterized by FT-IR, XRD, thermogravimetry analysis (TGA), SEM, and TEM. A_{ss} and average pore diameter were measured by the Brunauer–Emmett–Teller (BET) method. The potential of the chitosan-modified HSS material was evaluated for wound closure applications by conducting in vitro scratch assay. It was expected that in addition to the biological activity of chitosan, the HSS present in the system may allow gas exchanges and absorb wound exudates. Therefore, the newly developed material will be a best candidate for wound healing applications.

II. EXPERIMENTAL

A. Materials

Phenyl trimethoxysilane (PTMS) (97%), epichlorohydrin (99%), low-molecular-weight chitosan (mol wt 50,000–190,000 Da, deacetylated 75–85%), and dimethylformamide (DMF) were purchased from Sigma-Aldrich (St. Louis, Missouri). Other chemicals used in the synthesis such as HNO_3 and NH_4OH were of analytical purity.

B. Methodology

HSS nanoparticles were prepared as reported in our previous work.[19] Briefly, sol–gel method was adopted for developing HSS. PTMS was hydrolysed in an acidic medium (HNO_3), and the condensation of the HSS was performed in a basic medium (NH_4OH) [Fig. 1(a)]. The

https://doi.org/10.1557/jmr.2018.430 Published online by Cambridge University Press

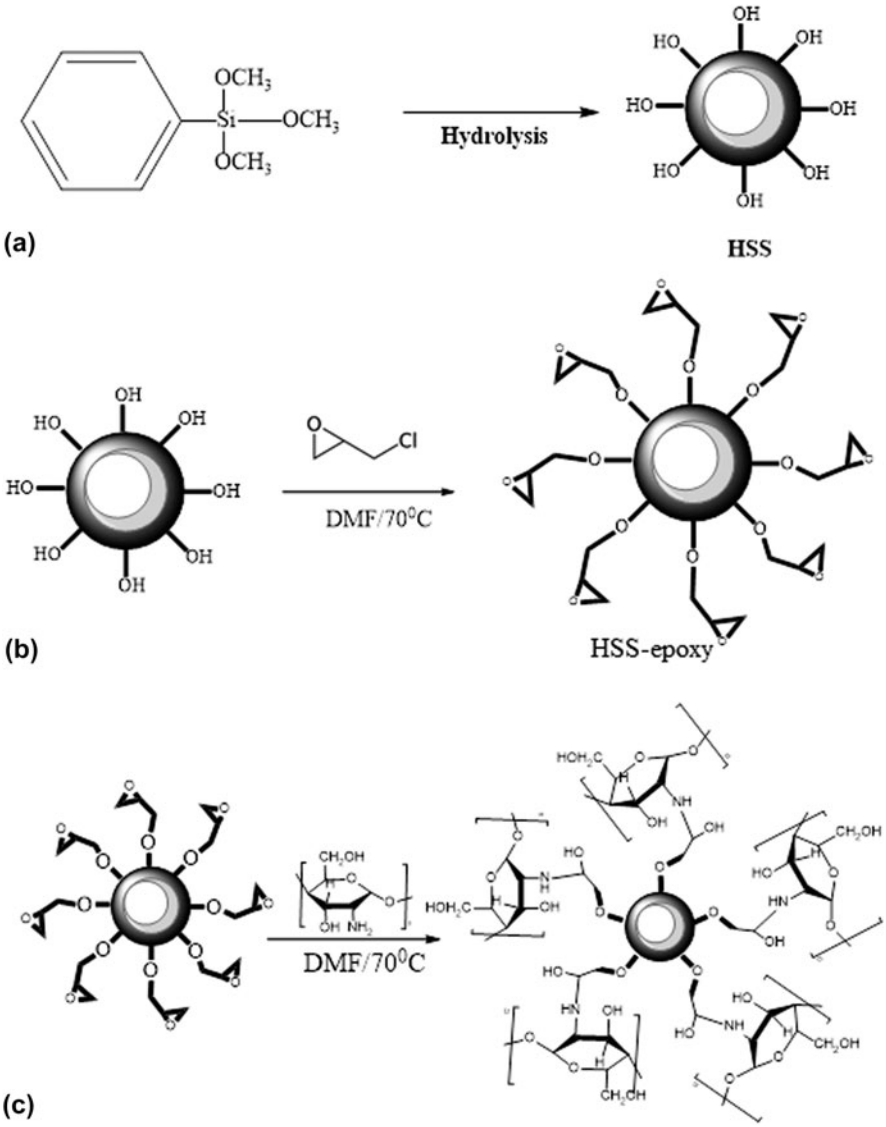


FIG. 1. Schematic representation of the preparation of chitosan-functionalized HSS nanoparticles: (a) preparation of HSS nanoparticle, (b) epoxidation of HSS surface, and (c) binding of chitosan to functionalized HSS.

precipitated nanoparticles were collected by a membrane filter and washed with water/ethanol mixture and then dried under vacuum.

For carrying out the epoxidation of HSS, a similar procedure described in the literature was used.[23] The HSS was mixed with DMF (0.1 g HSS in 10 mL DMF) and dispersed via ultrasonic bath for 20 min at room temperature. Then, excess epichlorohydrin was added dropwise to the solution at room temperature. Then, the reaction temperature was increased to 70 °C for 1 h. After the completion of reaction, the mixture was filtered and, to remove unreacted epichlorohydrin, was washed several times with ethyl alcohol–water (1:4) solution. Finally, modified HSSs were kept wet for further reaction [Fig. 1(b)].

The next step is the binding of chitosan on to the functionalized HSS surface [see Fig. 1(c)] via a ring-opening reaction of epoxy unit on HSS surfaces. HSS-epoxy was dispersed in acetic acid (0.2 g HSS-epoxy, 10 mL for 20%), and chitosan (w/w) in acetic acid (2 g chitosan, 30 mL for 20%) was added to the solution of epoxidized HSS at 70 °C and stirred for 24 h. HSS-epoxy-CHI was precipitated due to cross-linking. The precipitate was washed with water/methanol solution several times, filtered, and dried at 80 °C under vacuum. Different HSS-epoxy-CHI samples were prepared by varying the molar ratio of chitosan, i.e., 20, 40, and 60%. The formulation of the samples used in this study is given in Table I.

C. Characterization

FT-IR spectra were recorded on a Bruker Alpha-P in ATR (Bruker Corporation, Billerica, Massachusetts) in

https://doi.org/10.1557/jmr.2018.430 Published online by Cambridge University Press

TABLE I. Formulation of chitosan-functionalized HSS samples.

Sample code	% Composition of chitosan
HSS-epoxy-CHI-0	0%
HSS-epoxy-CHI-20	20%
HSS-epoxy-CHI-40	40%
HSS-epoxy-CHI-60	60%

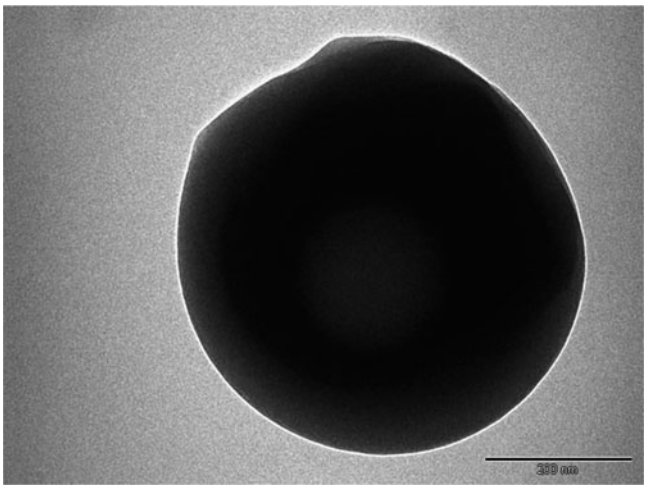


FIG. 2. TEM image of HSS nanoparticle.

the range of 4000–400 cm^{-1} (single-reflection diamond crystal). BET measurements were taken using an ASAP-2020 plus, accelerated surface area, and porosimetry (Micromeritics, Norcross, Georgia). Thermal stabilities of the samples were studied using TGA with a PerkinElmer Simultaneous Thermal Analyzer (STA) 6000 (PerkinElmer Inc., Waltham, Massachusetts). The samples (~10 mg) were heated from room temperature to 700 °C under N_2 atmosphere at a heating rate of 10 °C/min. XRD data were attained from a fully automated 9.0 kW anode rotating generator Rigaku Smart Lab X-Ray Diffractometer (Rigaku Corporation, Tokyo, Japan) with two-theta range of 0 to 70°. The surface morphology of the samples was detected using scanning electron microscopy (SEM; JEOL 7001 FESEM, JEOL Ltd., Tokyo, Japan). Samples were sputtered with gold for 150 s before the SEM measurements. For measuring the size of HSS, a transmission electron microscope (TEM; FEI, Morgagni, Czech Republic) was used.

1. In vitro wound healing (scratch) assay

NIH 3T3 fibroblasts cells were seeded in 12-well plates at 1×10^5 cells/well and grown until confluence in complete DMEM supplemented with 10% FBS, 2 mM L-glutamine, 100 U/mL penicillin, 100 μg/mL streptomycin, and 4.5 g/L glucose in a humidified chamber at 37 °C and 5% CO_2. To simulate a wound, a straight scratch was made in each well with a P200 pipette tip. The cell debris was removed, and the cells were treated with various formulations of nanoparticles for 24 h. The closure of the scratch was observed under the microscope at certain time intervals, i.e., 0, 14, and 21 h of exposure of scratch to the bionanocomposites. Digital images of cells were captured by a phase contrast microscope (Leica Microsystem, Weztlar, Germany). The closure of the scratch was calculated based on the width difference initially and after 14–21 h of treatment, using the ImageJ software (National Institutes of Health, Bethesda, Maryland) and expressed as a percentage of scratch closure.

III. RESULTS

A. BET surface area and TEM analysis of HSS nanoparticles

BET surface analysis is readily used to precisely measure the specific surface area (A_{ss}) of porous materials. In this study, the BET analysis was performed to measure the A_{ss} and pore size of HSSs. The product showed A_{ss} value of around 4.8 m^2/g. The Langmuir surface area was found to be around 8 m^2/g. The adsorption average pore diameter (4*V*/*A* by BET) was 10.180 nm.

Dimensions of HSS nanoparticles were measured with the help of a transmission electron microscope (TEM). TEM image (Fig. 2) showed that the size of HSS was ~400–450 nm, and the size of hollow was about 150 nm and thickness of cover was ~100 nm.

B. FT-IR analysis

Infrared spectra of chitosan, HSS, epoxy-functionalized HSS samples, and nanocomposites (HSS-epoxy-CHI-20, HSS-epoxy-CHI-40, HSS-epoxy-CHI-60) are shown in Fig. 3.

The spectra of HSS showed a strong absorption peak at 1092 cm^{-1} belonging to Si–O–Si asymmetric stretching. The peaks at 782 and 493 cm^{-1} could be assigned to symmetric stretching vibration of Si–O, and the peak at 936 cm^{-1} could be due to bending vibration of Si–OH.[24] A weak distinctive Si–OH stretching vibration was displayed at about 3600 cm^{-1}. The peak at 3100 cm^{-1} was attributed to asymmetrical stretching vibration of C–H groups of aromatic phenyl attached to HSS. These results demonstrated condensation product of PTMS to form HSS.

In the spectra of epoxy functionalized HSS, additional peaks were centered at 2900 cm^{-1} owing to the presence of methylene groups. Peak at 807 cm^{-1} indicated the presence of the epoxy group. In the epoxy-functionalized sample, the peak of Si–O–H showed slight change in its position and intensity, which indicates the participation of Si–OH in the epoxidation reaction.

Chitosan characteristic peaks were observed at 1650 cm^{-1} due to the amide group, 1568 cm^{-1} corresponding to N–H bending, 3288 cm^{-1} due to O–H,

https://doi.org/10.1557/jmr.2018.430 Published online by Cambridge University Press

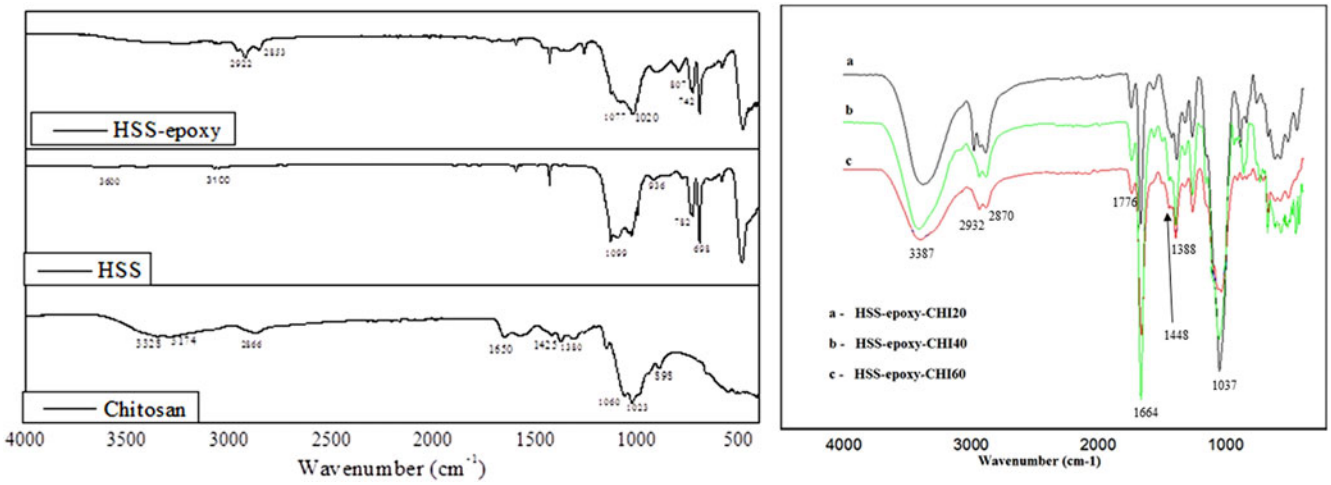


FIG. 3. FT-IR spectra of chitosan, HSS, epoxy-functionalized HSS, and HSS-epoxy-CHI nanocomposites.

2866 cm^{-1} C–H bending, 1425 cm^{-1} due to stretching vibrations of the amino group, 1154 cm^{-1} associated with C–O–C stretching, 1023 and 1060 cm^{-1} due to C–O-stretching, and 898 cm^{-1} due to glycosidic linkage.[25]

The spectra of HSS-epoxy-CHI nanocomposites showed distinct peaks of chitosan and silica. It can be observed that the peak in the region of 800 cm^{-1} associated with the epoxy group is absent in the chitosan-bound nanocomposites, which confirms the ring-opening reaction of epoxy. It is expected that amino group of chitosan is interacting with the epoxy group. The shift in the amino group peaks to lower frequency regions observed in the spectra of nanocomposites supports this assumption.

C. X-ray diffraction studies

The XRD patterns of the chitosan, HSS, and chitosan-functionalized HSS nanocomposites with a chitosan content of 40% and 60% are shown in Fig. 4. Pure chitosan showed a strong peak at $2\theta = 20.5°$ as reported in the literature.[26] The HSSs were comparatively amorphous in nature, and no highly crystalline peaks were observed, except one broad band around 22°.[27] For bionanocomposites, the intensity of this peak decreased, which indicates that chitosan-functionalized HSS nanocomposites were more amorphous in nature. However, among chitosan-functionalized HSS samples, the intensity of this broad peak increased with the increase in the percentage of chitosan in the composites.

D. Scanning electron microscopic analysis

The surface morphology of synthesized HSS and chitosan-functionalized HSS was analyzed using SEM. The SEM image of HSS [Fig. 5(a)] confirms the hollow nature of HSS. As evidenced from Fig. 2, the synthesized HSS showed an average diameter of 400–500 nm.

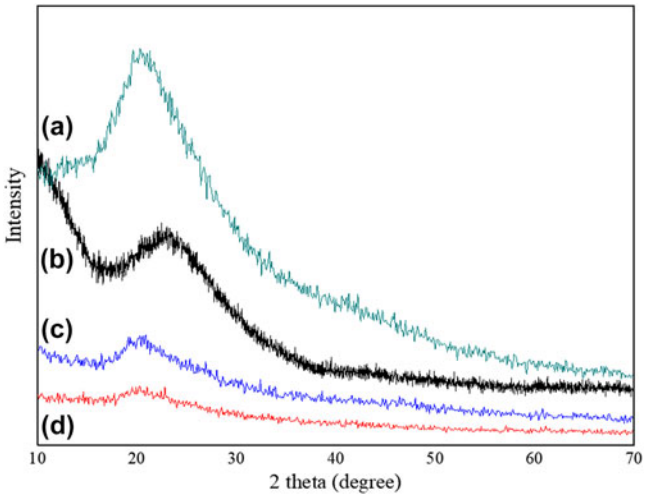


FIG. 4. XRD spectra of (a) pure chitosan, (b) HSS, (c) HSS-epoxy-CHI-60, and (d) HSS-epoxy-CHI-40.

Figure 5(b) shows the SEM image of chitosan-functionalized HSS (40% chitosan). It can be seen that HSS particles were homogeneously dispersed in chitosan and no phase separation was observed between chitosan and HSS after the modification of HSSs with chitosan via the ring-opening reaction of epoxy. As expected, the dimension of chitosan-functionalized HSS nanoparticles increased compared with pure HSS because of the presence of chitosan coating on the surface of HSS.

E. Thermal analysis

TGA plots of chitosan-functionalized HSS samples are shown in Fig. 6, which show similar pattern, and only a slight variation in thermal stability is observed. Chitosan usually follows a two-step degradation profile: a small weight loss within the temperature range 30–180 °C due to the evaporation of absorbed water and small molecules; and a major weight loss between 250 and 600 °C

https://doi.org/10.1557/jmr.2018.430 Published online by Cambridge University Press

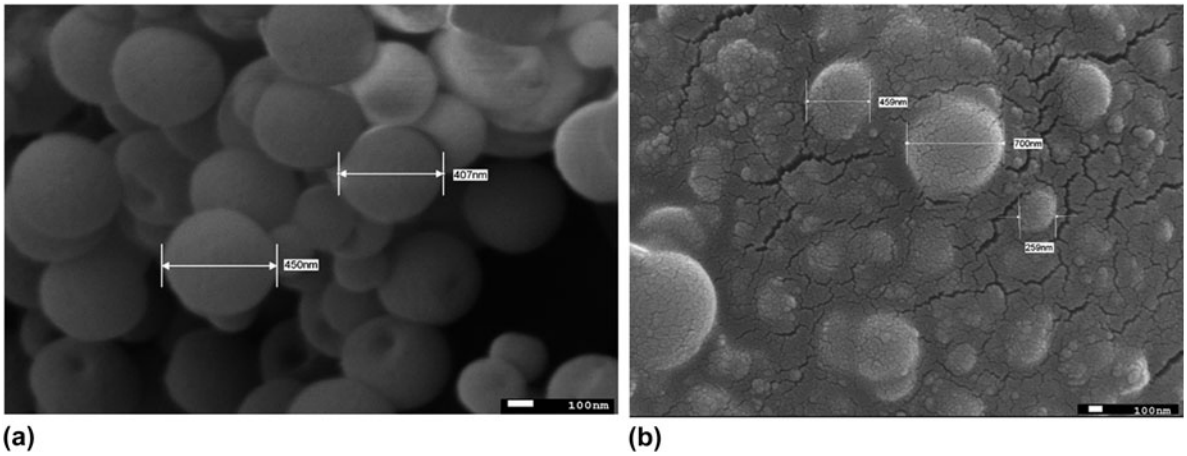


FIG. 5. SEM image of (a) HSS nanoparticle and (b) HSS-epoxy-CHI-40 nanocomposite.

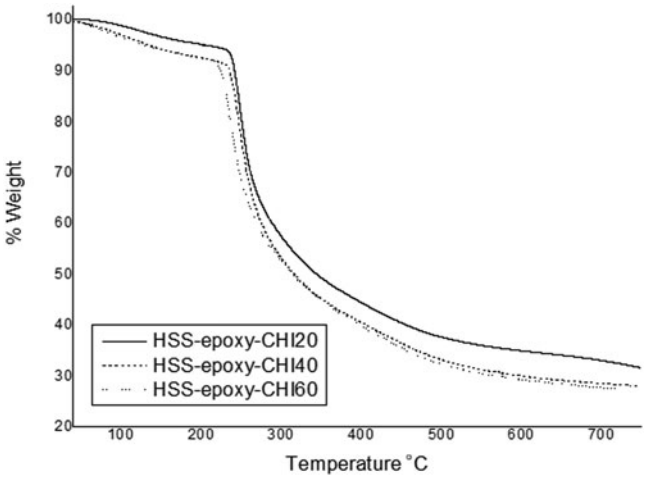


FIG. 6. TGA curves of chitosan-functionalized HSS samples.

due to the decomposition of chitosan polymer chains and the degradation of phenyl groups of HSS.[28] It is interesting to note that chitosan-functionalized HSS samples exhibited higher thermal stability at lower temperatures when compared to HSS-epoxy sample that contained no chitosan. When the plots of nanocomposites were compared, there were small variations in the initial weight loss of the chitosan-functionalized samples due to the variation in the moisture content in the nanocomposites. Samples with high percentage of chitosan showed greater weight loss. The residue content of the samples was proportionate to the chitosan content in it. Sample prepared with low chitosan content showed higher residue content and samples with high chitosan content showed less residue content due to the complete degradation of the chitosan molecules.

F. In vitro wound healing (scratch) assay

Skin is the largest body organ, which protects our body by acting as a barrier and preventing harmful pathogens from entering our body. However, a wound can occur on the skin either by a physical, chemical, or thermal damage. Wounds and burns are a serious problem in health care. The production process of wound healing is a complex system that involves the regeneration of the damaged tissues and replacement of lost tissues. Wound healing process mainly involves four phases: hemostasis, inflammation, proliferation, and remodelling.[29] To investigate the wound healing potential of chitosan-functionalized HSS nanoparticles, each of the newly synthesized formulations in DMSO was tested using in vitro wound healing assay. The wound was simulated by introducing a straight scratch in a confluent culture of NIH 3T3 fibroblasts. The percent closure was observed and calculated 14 and 21 h later. Fourteen hours after introducing a scratch and treating with different nanocomposites, 100 μg/mL of HSS formulation loaded with 60% chitosan had significantly higher percent closure of about 70%, that is, healing, compared to the untreated controls with average percent closure of about 30% [see Fig. 7(a)]. All of the remaining nanocomposites showed slightly higher but not statistically significant increase in percent closure of the initial scratch. Twenty-one hours after introducing a scratch and exposure to different ratios of nanocomposites, the average percent closure of untreated control is increased to about 50%. However, scratch exposed to different amounts of HSS showed average percent closure higher than the controls with most of the nanocomposites having a statistically higher increase in percent closure [see Fig. 7(b)]. This is quite expected due to biological activity of chitosan and the hollow nature of silica which permits exudates absorption and gas exchange. Similar to the 14 h treatment period, the 100 μg/mL of HSS formulation loaded with 60% chitosan had the highest percent closure of about 90%.

Figure 8 shows the photomicrographs of scratch analysis at various time intervals, i.e., at 0, 14, and 21 h after the scratch and exposure to different chitosan–HSS

https://doi.org/10.1557/jmr.2018.430 Published online by Cambridge University Press

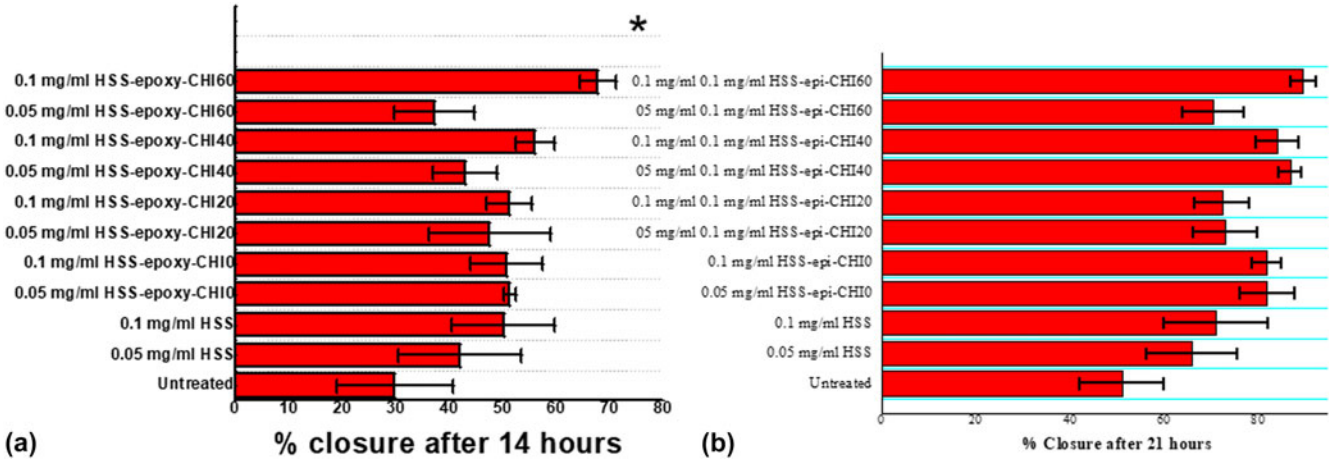


FIG. 7. Wound healing potential of novel HSS-based formulations in in vitro wound healing assay (a) 14 and (b) 21 h after the scratch and exposure to different formulations (mean ± SEM, $n = 4$ from a total of four repeated experiments, *: $P < 0.05$ and **: $P < 0.01$ compared with the untreated controls).

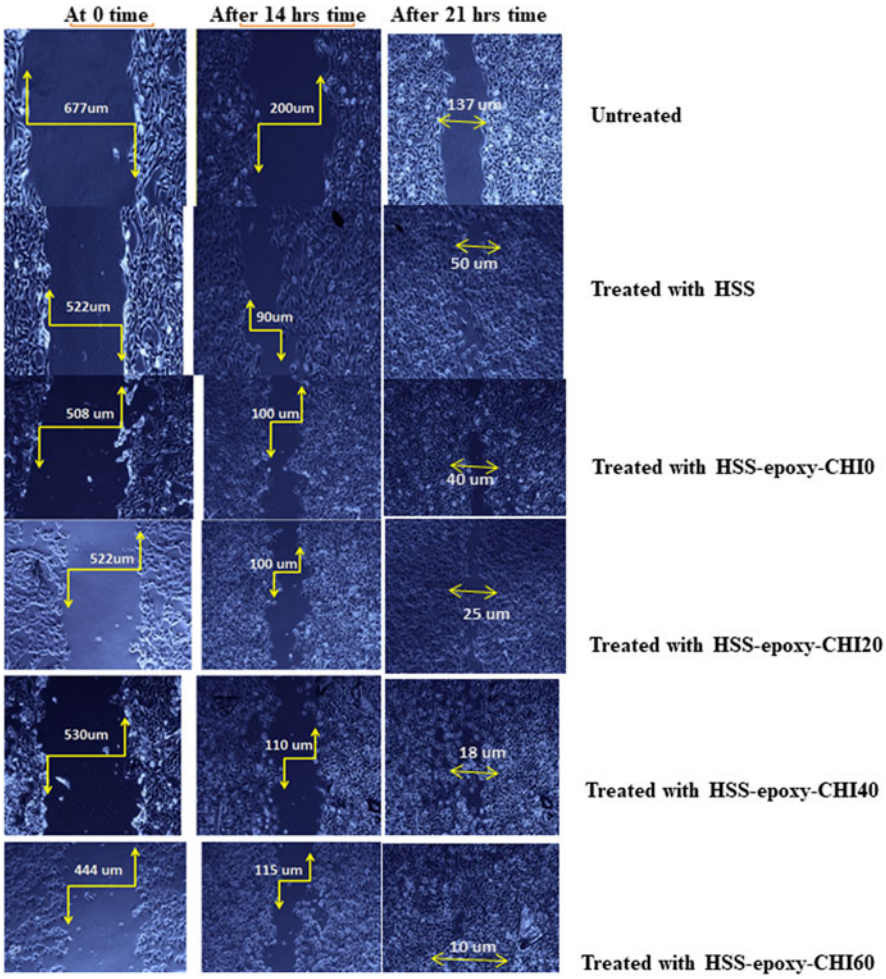


FIG. 8. Photomicrographs of in vitro scratch test at 0, 14, and 21 h after the scratch and exposure to different chitosan–HSS-based formulations (mean ± SEM, $n = 4$ from a total of four repeated experiments, *: $P < 0.05$ and **: $P < 0.01$ compared with the untreated controls) (100× magnification).

https://doi.org/10.1557/jmr.2018.430 Published online by Cambridge University Press

formulations (concentration—0.1 mg/mL). Compared with the untreated scratch, greater percent closure was observed for the scratch treated with HSS–chitosan formulations. It was observed that as the chitosan content in the formulation increases, percent wound closure increases. Among the different formulations studied, formulation with 60% chitosan content showed greater wound closure. It can be seen that, in all cases, as the exposure time increases, more closure can be achieved. Compared with 14-h-treated samples, more percent closure was observed after 21 h.

Clearly, in vitro scratch assay was used as a tool to investigate the wound healing potential of the novel composite materials. Percentage closure of the scratch was measured after certain time intervals of exposure to nanocomposites. Greater percentage closure was observed for samples with greater content of chitosan, because of the specific biological features of bionanocomposite. When the time of exposure increased, greater closure was observed. The newly developed material could create a better environment for the wound closure.

IV. CONCLUSIONS

Chitosan-functionalized hollow silica nanoparticles were prepared and characterized by different techniques such as FT-IR, TGA, XRD, SEM, and TEM. BET analysis of pristine HSS was performed, and A_{ss} value was found to be around 4.8 m^2/g and the adsorption average pore diameter was found to be 10.18 nm. Binding of chitosan on the HSS nanoparticle was confirmed using FT-IR analysis and SEM analysis. These novel biocompatible nanoparticles were tested for application in wound healing by carrying out in vitro scratch assay using NIH 3T3 fibroblast cells. Out of the analyzed nanocomposites, HSS-epoxy-CHI-60 bionanocomposite exhibited better performance. About 70% wound closure was observed for this sample after 14 h of exposure, and 90% wound closure was observed after 21 h of treatment. The synergic effect of chitosan and HSS leads to better performance of these materials. From the results it can be seen that wound healing ability of the samples is proportionate to the chitosan content in the samples, concentration of nanoparticles formulation, and the exposure time. Scratch exposed to higher concentration of chitosan nanocomposites showed wound closure to a greater extent. It can be summarized that the newly developed functionalized materials have great potential for application in wound care.

ACKNOWLEDGMENT

This work was supported by Institute for Research and Medical Consultations (IRMC) - IAU.

REFERENCES

1. R.A.A. Muzzarelli: Chitins and chitosans for the repair of wounded skin, nerve, cartilage and bone. *Carbohydr. Polym.* **76**, 167 (2009).
2. S. Ahmed, M. Jayachandran, M.A. Qureshi, and S.M. Ikram: Chitosan based dressings for wound care. *Immunochem. Immunopathol.* **1**, 1 (2015).
3. S. Ahmed and S. Ikram: Chitosan based scaffolds and their applications in wound healing. *Achiev. Life Sci.* **10**, 27 (2016).
4. Y. Zhou, D. Yang, X. Chen, Q. Xu, F. Lu, and J. Nie: Electrospun water-soluble carboxyethyl chitosan/poly(vinyl alcohol) nanofibrous membrane as potential wound dressing for skin regeneration. *Biomacromolecules* **9**, 349 (2008).
5. Y. Zhou, H. Yang, X. Liu, J. Mao, S. Gu, and W. Xu: Electrospinning of carboxyethyl chitosan/poly(vinyl alcohol)/silk fibroin nanoparticles for wound dressings. *Int. J. Biol. Macromol.* **53**, 88 (2013).
6. V.C. Nguyen, V.B. Nguyen, and M.F. Hsieh: Curcumin-loaded chitosan/gelatin composite sponge for wound healing application. *Int. J. Polym. Sci.* **2013**, 1 (2013).
7. M.P. Ribeiro, A. Espiga, D. Silva, P. Baptista, J. Henriques, C. Ferreira, J.C. Silva, J.P. Borges, E. Pires, P. Chaves, and I.J. Correia: Development of a new chitosan hydrogel for wound dressing. *Wound Repair Regen.* **17**, 817 (2009).
8. X. Zhang, D. Yang, and J. Nie: Chitosan/polyethylene glycol diacrylate films as potential wound dressing material. *Int. J. Biol. Macromol.* **43**, 456 (2008).
9. Z. Deng, Z. Zhen, X. Hu, S. Wu, Z. Xu, and P.K. Chu: Hollow chitosan-silica nanospheres as pH-sensitive targeted delivery carriers in breast cancer therapy. *Biomaterials* **32**, 4976 (2011).
10. A. Liberman, N. Mendez, W.C. Trogler, and A.C. Kummel: Synthesis and surface functionalization of silica nanoparticles for nanomedicine. *Surf. Sci. Rep.* **69**, 132 (2014).
11. R. Gui, Y. Wang, and J. Sun: Embedding fluorescent mesoporous silica nanoparticles into biocompatible nanogels for tumor cell imaging and thermo/pH-sensitive in vitro drug release. *Colloids Surf., B* **116**, 518 (2014).
12. W.T. Liu, Y. Yang, P.H. Shen, X.J. Gao, S.Q. He, H. Liu, and C.S. Zhu: Facile and simple preparation of pH-sensitive chitosan-mesoporous silica nanoparticles for future breast cancer treatment. *Express Polym. Lett.* **9**, 1068 (2015).
13. J. Jiao, X. Li, S. Zhang, J. Liu, D. Di, Y. Zhang, Q. Zhao, and S. Wang: Redox and pH dual-responsive PEG and chitosan-conjugated hollow mesoporous silica for controlled drug release. *Mater. Sci. Eng., C* **67**, 26 (2016).
14. Y. Bao, C. Shi, T. Wang, X. Li, and J. Ma: Recent progress in hollow silica: Template synthesis, morphologies and applications. *Microporous Mesoporous Mater.* **227**, 121 (2016).
15. A. Chen, Y. Yu, H. Lv, Y. Zhang, T. Xing, and Y. Yu: Synthesis of hollow mesoporous silica spheres and carambola-like silica materials with a novel resin sphere as template. *Mater. Lett.* **135**, 43 (2014).
16. Y. Dong, E. Wang, L. Yu, R. Wang, Y. Zhu, Y. Fu, and Q.Q. Ni: Self-templated route to synthesis bowl-like and deflated balloon-like hollow silica spheres. *Mater. Lett.* **206**, 150 (2017).
17. H.J. Hah, J.S. Kim, B.J. Jeon, S.M. Koo, and Y.E. Lee: Simple preparation of monodisperse hollow silica particles without using templates. *Chem. Commun.* **14**, 1712 (2003).
18. Q. Wang, Y. Liu, and H. Yan: Mechanism of a self-templating synthesis of monodispersed hollow silica nanospheres with tunable size and shell thickness. *Chem. Commun.* **23**, 2339 (2007).
19. A. Aslan, A.M. Soydan, and A. Bozkurt: Synthesis and characterization of novel multifunctional polymer grafted hollow silica spheres. *J. Mater. Res.* **30**, 2408 (2015).
20. F. Chen and Y. Zhu: Chitosan enclosed mesoporous silica nanoparticles as drug nano-carriers: Sensitive response to the narrow pH range. *Microporous Mesoporous Mater.* **150**, 83 (2012).
21. X. Sun, Z. Tang, M. Pan, Z. Wang, H. Yang, and H. Liu: Chitosan/kaolin composite porous microspheres with high hemostatic efficacy. *Carbohydr. Polym.* **177**, 135 (2017).

https://doi.org/10.1557/jmr.2018.430 Published online by Cambridge University Press

22. Y. Wang, Y. Fu, J. Li, Y. Mu, X. Zhang, K. Zhang, M. Liang, C. Feng, and X. Chen: Multifunctional chitosan/dopamine/diatom-biosilica composite beads for rapid blood coagulation. *Carbohydr. Polym.* **200**, 6 (2018).
23. C. Alzina, N. Sbirrazzuoli, and A. Mija: Epoxy amine based nanocomposites reinforced by silica nanoparticles. Relationships between morphologic aspects, cure kinetics, and thermal properties. *J. Phys. Chem. C*. **115**, 22789 (2011).
24. X. Xiang, S. Ding, H. Suo, C. Xu, Z. Gao, and Y. Hu: Fabrication of chitosan-mesoporous silica SBA-15 nanocomposites via functional ionic liquid as the bridging agent for PPL immobilization. *Carbohydr. Polym.* **182**, 245 (2018).
25. F. Al-Sagheer and S. Muslim: Thermal and mechanical properties of chitosan/hybrid composites. *J. Nanomater.* **2010**, 490679 (2010).
26. C. Flores, M. Lopez, N. Tabary, C. Neut, F. Chai, D. Betbeder, C. Herkt, F. Cazaux, V. Gaucher, B. Martel, and N. Blanchemain: Preparation and characterization of novel chitosan and β-cyclodextrin polymer sponges for wound dressing applications. *Carbohydr. Polym.* **173**, 535 (2017).
27. J.J. Chen, H.J. Li, X.H. Zhou, E.Z. Li, Y. Wang, Y.L. Guo, and Z.S. Feng: Efficient synthesis of hollow silica microspheres useful for porous silica ceramics. *Ceram. Int.* **43**, 13907 (2017).
28. Y. Zhao, N. Yan, and M.W. Feng: Thermal degradation characteristics of phenol-formaldehyde resins derived from beetle infested pine barks. *Thermochim. Acta* **555**, 46 (2013).
29. H. Sinno and S. Prakash: Complements and the wound healing cascade: An updated review. *Plast. Surg. Int*. **2013**, 146764 (2013).

Supplementary Material

To view supplementary material for this article, please visit https://doi.org/10.1557/jmr.2018.430.

https://doi.org/10.1557/jmr.2018.430 Published online by Cambridge University Press